

# Searching for Odderon in Central Exclusive Processes at the LHC\*

PIOTR LEBIEDOWICZ

Institute of Nuclear Physics Polish Academy of Sciences,  
ul. Radzikowskiego 152, PL-31-342 Kraków, Poland

There seem to be recently an evidence for  $C = -1$  odderon exchange in proton-proton elastic scattering at high energies. Here we discuss three different central-exclusive-production processes  $pp \rightarrow pp(\phi \rightarrow K^+K^-)$ ,  $pp \rightarrow pp(\phi \rightarrow \mu^+\mu^-)$ , and  $pp \rightarrow pp\phi\phi \rightarrow ppK^+K^-K^+K^-$ , as a possible source of information for soft odderon exchange. The theoretical results are calculated within the tensor-pomeron and vector-odderon model for soft reactions. We include absorptive corrections at the amplitude level. To describe the low-energy data measured in the past by the WA102 collaboration we consider also subleading processes with reggeized vector-meson exchanges and reggeons. We discuss possible evidences for odderon exchange at the low energies and try to make predictions at the LHC.

## 1. Introduction

The odderon exchange became recently topical again. So far there is no unambiguous experimental evidence for the odderon ( $\mathbb{O}$ ), the charge conjugation  $C = -1$  counterpart of the  $C = +1$  pomeron ( $\mathbb{P}$ ), introduced on theoretical grounds in [1, 2]. The odderon was predicted in QCD as a colourless  $C$ -odd three-gluon bound state exchange [3, 4]. A hint of the odderon was seen in ISR results [5] as a small difference between the differential cross sections of elastic proton-proton ( $pp$ ) and proton-antiproton ( $p\bar{p}$ ) scattering in the diffractive dip region at  $\sqrt{s} = 53$  GeV. The interpretation of this difference is, however, complicated due to non-negligible contributions from secondary reggeons. Recently the TOTEM Collaboration has published data from high-energy elastic proton-proton scattering experiments at the LHC [6, 7]. The interpretation of these results is controversial at the moment. Some authors claim for instance that the  $\rho$  measurements show

---

\* Presented at XXVI Cracow EIPHANY Conference, LHC Physics: Standard Model and Beyond, 7-10 January 2020

that there must be an odderon effect at  $t = 0$  [8]. But other authors find that no odderon contribution is needed at  $t = 0$  [9, 10, 11].

As was discussed in [12] exclusive diffractive  $J/\psi$  and  $\phi$  production from the pomeron-odderon fusion in high-energy  $pp$  and  $p\bar{p}$  collisions is a direct probe for a possible odderon exchange. Exclusive production of heavy vector mesons,  $J/\psi$  and  $\Upsilon$ , from the pomeron-odderon and the pomeron-photon fusion in the pQCD  $k_t$ -factorization approach was discussed in [13]. However, so far in no one of the exclusive reactions a clear identification of the odderon was found experimentally.

A possible probe of the odderon is photoproduction of  $C = +1$  mesons [14, 15]. At sufficiently high energies only odderon and photon exchange contribute to these reactions. Photoproduction of the pseudoscalars  $\pi^0$ ,  $\eta$ ,  $\eta'$ ,  $\eta_c$ , and of the tensor  $f_2(1270)$  in  $ep$  scattering at high energies was discussed in [16, 17, 18, 19, 20]. For a nice review of odderon physics see [21]. In [24] the measurement of the exclusive  $\eta_c$  production in nuclear collisions was discussed. Recently, the possibility of probing the odderon in ultraperipheral proton-ion collisions was considered [22, 23]. The situation of the odderon in this context is also not obvious and requires further studies.

In [25] the tensor-pomeron and vector-odderon concept was introduced for soft reactions. In this approach, the  $C = +1$  pomeron and the reggeons  $\mathbb{R}_+ = f_{2\mathbb{R}}, a_{2\mathbb{R}}$  are treated as effective rank-2 symmetric tensor exchanges while the  $C = -1$  odderon and the reggeons  $\mathbb{R}_- = \omega_{\mathbb{R}}, \rho_{\mathbb{R}}$  are treated as effective vector exchanges. Applications of the tensor-pomeron and vector-odderon ansatz were given for photoproduction of pion pairs in [26] and for a number of central-exclusive-production (CEP) reactions in  $pp$  collisions in [27, 28, 29, 30, 31]. Also contributions from the subleading exchanges,  $\mathbb{R}_+$  and  $\mathbb{R}_-$ , were discussed in these works. As an example, for the  $pp \rightarrow ppp\bar{p}$  reaction [28] the contributions involving the odderon are expected to be small since its coupling to the proton is very small. We have predicted asymmetries in the (pseudo)rapidity distributions of the centrally produced antiproton and proton. The asymmetry is caused by interference effects of the dominant  $(\mathbb{P}, \mathbb{P})$  with the subdominant  $(\mathbb{O} + \mathbb{R}_-, \mathbb{P} + \mathbb{R}_+)$  and  $(\mathbb{P} + \mathbb{R}_+, \mathbb{O} + \mathbb{R}_-)$  exchanges. We find for the odderon only very small effects, roughly a factor 10 smaller than the effects due to reggeons.

In [32] the helicity structure of small- $|t|$  proton-proton elastic scattering was considered in three models for the pomeron: tensor, vector, and scalar. Only the tensor ansatz for the pomeron was found to be compatible with the high-energy experiment on polarized  $pp$  elastic scattering [33]. In [34] the authors, using combinations of two tensor-type pomerons (a soft one and a hard one) and the  $\mathbb{R}_+$ -reggeon exchange, successfully described low- $x$  deep-inelastic lepton-nucleon scattering and photoproduction.

In this talk we considered three exclusive processes in proton-proton

collisions  $pp \rightarrow pp(\phi \rightarrow K^+K^-)$ ,  $pp \rightarrow pp(\phi \rightarrow \mu^+\mu^-)$ , and  $pp \rightarrow pp(\phi\phi \rightarrow K^+K^-K^+K^-)$  in the nonperturbative tensor-pomeron and vector-odderon approach. These processes were discussed in details in Refs. [30, 31].

## 2. A sketch of formalism

For single  $\phi$  production we include processes shown in Fig. 1. For high energies and central  $\phi \equiv \phi(1020)$  production we expect the reaction  $pp \rightarrow pp\phi$  to be dominated by the fusion processes  $\gamma\mathbb{P} \rightarrow \phi$  and  $\mathbb{O}\mathbb{P} \rightarrow \phi$ . For the first process all couplings are, in essence, known. For the odderon-exchange process we shall use the ansätze from [25] and we shall try to get information on the odderon parameters and couplings from the comparison to the WA102 data for the  $pp \rightarrow pp\phi$  and  $pp \rightarrow pp\phi\phi$  reactions. At the relatively low center-of-mass energy of the WA102 experiment,  $\sqrt{s} = 29.1$  GeV, we have to include also subleading contributions with vector-meson (or reggeon) exchanges discussed in details in [31].

In the diffractive production of  $\phi$  meson pairs, it is possible to have pomeron-pomeron fusion with intermediate  $\hat{t}/\hat{u}$ -channel odderon exchange [30]; see the first diagram in Fig. 2. Thus, the reaction is a good candidate for the  $\mathbb{O}$ -exchange searches, as it does not involve the coupling of the odderon to the proton (the  $\mathbb{O}$ - $\mathbb{P}$ - $\mathbb{O}$  contribution is negligibly small).

As an example, we consider the reaction

$$p(p_a) + p(p_b) \rightarrow p(p_1) + [\phi(p_{34}) \rightarrow K^+(p_3) + K^-(p_4)] + p(p_2), \quad (1)$$

where  $p_{a,b}$ ,  $p_{1,2}$  denote the four-momenta of the protons and  $p_{3,4}$  denote the four-momenta of the  $K$  mesons, respectively. The kinematic variables are

$$\begin{aligned} p_{34} &= p_3 + p_4, & q_1 &= p_a - p_1, & q_2 &= p_b - p_2, \\ s &= (p_a + p_b)^2 = (p_1 + p_2 + p_{34})^2, \\ t_1 &= q_1^2, & t_2 &= q_2^2, & s_1 &= (p_1 + p_{34})^2, & s_2 &= (p_2 + p_{34})^2. \end{aligned} \quad (2)$$

The Born-level amplitude for the diffractive production of the  $\phi(1020)$  via odderon-pomeron fusion, see diagram (a) in Fig. 1, can be written as

$$\begin{aligned} \mathcal{M}_{pp \rightarrow ppK^+K^-}^{(\mathbb{O}\mathbb{P})} &= (-i)\bar{u}(p_1, \lambda_1) i\Gamma_{\mu}^{(\mathbb{O}pp)}(p_1, p_a) u(p_a, \lambda_a) \\ &\times i\Delta^{(\mathbb{O})\mu\rho_1}(s_1, t_1) i\Gamma_{\rho_1\rho_2\alpha\beta}^{(\mathbb{P}\mathbb{O}\phi)}(-q_1, p_{34}) i\Delta^{(\phi)\rho_2\kappa}(p_{34}) i\Gamma_{\kappa}^{(\phi KK)}(p_3, p_4) \\ &\times i\Delta^{(\mathbb{P})\alpha\beta,\delta\eta}(s_2, t_2) \bar{u}(p_2, \lambda_2) i\Gamma_{\delta\eta}^{(\mathbb{P}pp)}(p_2, p_b) u(p_b, \lambda_b). \end{aligned} \quad (3)$$

The effective propagator and the proton vertex function for tensorial pomeron are as follows [25]:

$$i\Delta_{\mu\nu,\kappa\lambda}^{(\mathbb{P})}(s, t) = \frac{1}{4s} \left( g_{\mu\kappa}g_{\nu\lambda} + g_{\mu\lambda}g_{\nu\kappa} - \frac{1}{2}g_{\mu\nu}g_{\kappa\lambda} \right) (-is\alpha'_{\mathbb{P}})^{\alpha_{\mathbb{P}}(t)-1}, \quad (4)$$

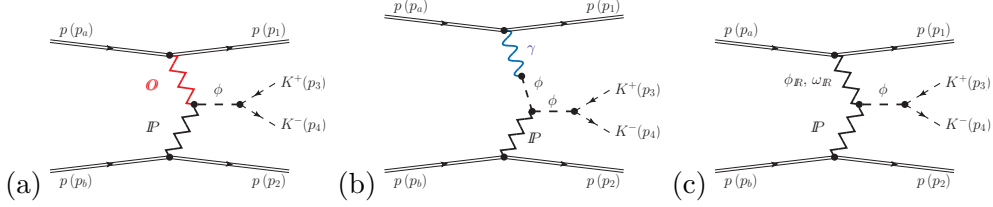


Fig. 1. Some Born-level diagrams included in the analysis of single  $\phi$  production: (a) odderon-pomeron fusion process; (b) photoproduction ( $\gamma\mathbb{P}$  fusion) process; (c) reggeon-pomeron fusion processes. There are also the corresponding diagrams with the rôle of the protons interchanged,  $(p(p_a), p(p_1)) \leftrightarrow (p(p_b), p(p_2))$ .

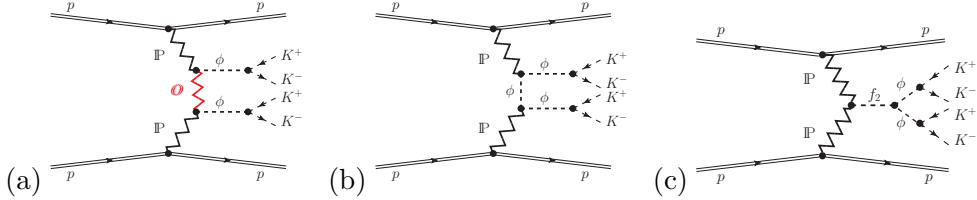


Fig. 2. The Born-level diagrams for double pomeron central exclusive  $\phi\phi$  production and their decays into  $K^+K^-K^+K^-$ : (a) continuum  $\phi\phi$  production via an intermediate odderon exchange; (b) continuum via reggeized  $\phi$ -meson exchange; (c)  $\phi\phi$  production via an  $f_2$  resonance. Other resonances, e.g. of  $f_0$ - and  $\eta$ -type, can also contribute here; see Ref. [30].

$$i\Gamma_{\mu\nu}^{(\mathbb{P}pp)}(p', p) = -i3\beta_{\mathbb{P}NN}F_1((p' - p)^2) \times \left\{ \frac{1}{2} [\gamma_\mu(p' + p)_\nu + \gamma_\nu(p' + p)_\mu] - \frac{1}{4}g_{\mu\nu}(\not{p}' + \not{p}) \right\}, \quad (5)$$

where  $\beta_{\mathbb{P}NN} = 1.87 \text{ GeV}^{-1}$  and  $t = (p' - p)^2$ . For simplicity we use the electromagnetic Dirac form factor  $F_1(t)$  of the proton. The pomeron trajectory  $\alpha_{\mathbb{P}}(t)$  is assumed to be of standard linear form (see, e.g., [35]):  $\alpha_{\mathbb{P}}(t) = \alpha_{\mathbb{P}}(0) + \alpha'_{\mathbb{P}} t$ ,  $\alpha_{\mathbb{P}}(0) = 1.0808$ ,  $\alpha'_{\mathbb{P}} = 0.25 \text{ GeV}^{-2}$ .

Our ansatz for the  $C = -1$  odderon follows (3.16), (3.17) and (3.68), (3.69) of [25]:

$$i\Delta_{\mu\nu}^{(\mathbb{O})}(s, t) = -ig_{\mu\nu} \frac{\eta_{\mathbb{O}}}{M_0^2} (-is\alpha'_{\mathbb{O}})^{\alpha_{\mathbb{O}}(t)-1}, \quad (6)$$

$$i\Gamma_{\mu}^{(\mathbb{O}pp)}(p', p) = -i3\beta_{\mathbb{O}pp} M_0 F_1((p' - p)^2) \gamma_{\mu}, \quad (7)$$

where  $\eta_{\mathbb{O}}$  is a parameter with value  $\eta_{\mathbb{O}} = \pm 1$ ;  $M_0 = 1 \text{ GeV}$  is inserted for dimensional reasons. We assumed for the odderon trajectory  $\alpha_{\mathbb{O}}(t) = \alpha_{\mathbb{O}}(0) + \alpha'_{\mathbb{O}} t$ . In our calculations we shall choose as default values  $\alpha_{\mathbb{O}}(0) = 1.05$ ,  $\alpha'_{\mathbb{O}} = 0.25 \text{ GeV}^{-2}$ , and  $\eta_{\mathbb{O}} = -1$ ; see [31]. We assumed  $\beta_{\mathbb{O}pp} = 0.1 \beta_{\mathbb{P}NN}$ .

For the  $\mathbb{P}\mathbb{O}\phi$  vertex we use an ansatz analogous to the  $\mathbb{P}\phi\phi$  vertex; see (3.48)–(3.50) of [30]. We get then with  $(-q_1, \rho_1)$  and  $(p_{34}, \rho_2)$  the outgoing oriented momenta and the vector indices of the odderon and the  $\phi$  meson, respectively, and  $\alpha\beta$  the pomeron indices,

$$i\Gamma_{\rho_1\rho_2\alpha\beta}^{(\mathbb{P}\mathbb{O}\phi)}(-q_1, p_{34}) = i \left[ 2 a_{\mathbb{P}\mathbb{O}\phi} \Gamma_{\rho_2\rho_1\alpha\beta}^{(0)}(p_{34}, -q_1) - b_{\mathbb{P}\mathbb{O}\phi} \Gamma_{\rho_2\rho_1\alpha\beta}^{(2)}(p_{34}, -q_1) \right] \times F_M(q_2^2) F_M(q_1^2) F^{(\phi)}(p_{34}^2). \quad (8)$$

Here we use the relations (3.20) of [25] and as in (3.49) of [30] we take the factorised form for the  $\mathbb{P}\mathbb{O}\phi$  form factor; see [31]. The coupling parameters  $a_{\mathbb{P}\mathbb{O}\phi}$ ,  $b_{\mathbb{P}\mathbb{O}\phi}$  in (8) and the cut-off parameter  $\Lambda_{0, \mathbb{P}\mathbb{O}\phi}^2$  in  $F_M(t) = 1/(1 - t/\Lambda_{0, \mathbb{P}\mathbb{O}\phi}^2)$  could be adjusted to experimental data. The WA102 data allow us to determine the respective coupling constants as  $a_{\mathbb{P}\mathbb{O}\phi} = -0.8 \text{ GeV}^{-3}$ ,  $b_{\mathbb{P}\mathbb{O}\phi} = 1.6 \text{ GeV}^{-1}$ , and  $\Lambda_{0, \mathbb{P}\mathbb{O}\phi}^2 = 0.5 \text{ GeV}^2$ ; see Sec. IV A of [31]. We have checked that these parameters are compatible with our analysis of the WA102 data for the  $pp \rightarrow pp\phi\phi$  reaction in [30].

The full form of the vector-meson propagator is given by (3.2) of [25]. Here we take the simple Breit-Wigner expression as discussed in [29]. For the  $\phi KK$  vertex we follow (4.24)–(4.26) of [29]. For the details see Ref. [31].

To give the full physical amplitude we should include absorptive corrections to the Born amplitudes; see e.g. [36]. The full amplitude includes the  $pp$ -rescattering corrections in the eikonal approximation is written as

$$\mathcal{M} = \mathcal{M}^{\text{Born}} + \mathcal{M}^{\text{abs.}}, \quad (9)$$

$$\mathcal{M}^{\text{abs.}}(s, \mathbf{p}_{1t}, \mathbf{p}_{2t}) = \frac{i}{8\pi^2 s} \int d^2\mathbf{k}_t \mathcal{M}^{\text{Born}}(s, \tilde{\mathbf{p}}_{1t}, \tilde{\mathbf{p}}_{2t}) \mathcal{M}_{\text{el}}^{(\mathbb{P})}(s, -\mathbf{k}_t^2), \quad (10)$$

where  $\tilde{\mathbf{p}}_{1t} = \mathbf{p}_{1t} - \mathbf{k}_t$  and  $\tilde{\mathbf{p}}_{2t} = \mathbf{p}_{2t} + \mathbf{k}_t$ .  $\mathcal{M}_{\text{el}}^{(\mathbb{P})}$  is the elastic  $pp$ -scattering amplitude with the momentum transfer  $t = -\mathbf{k}_t^2$ .

### 3. Results

It is very difficult to describe the WA102 data from [38] for the  $pp \rightarrow pp\phi$  reaction including the  $\gamma\mathbb{P}$ -fusion mechanism only. The result of our analysis is shown in Fig. 3. Inclusion of the odderon-exchange contribution significantly improves the description of the  $pp$  azimuthal correlations and the  $dP_t$  “glueball-filter variable” dependence of  $\phi$  CEP measured by WA102; see the discussion in [31]. The absorption effects are included here and in the calculations presented below. To describe the low-energy data more accurately we consider also subleading fusion processes. Here we present results for the approach II of [31]. We can see that the complete results

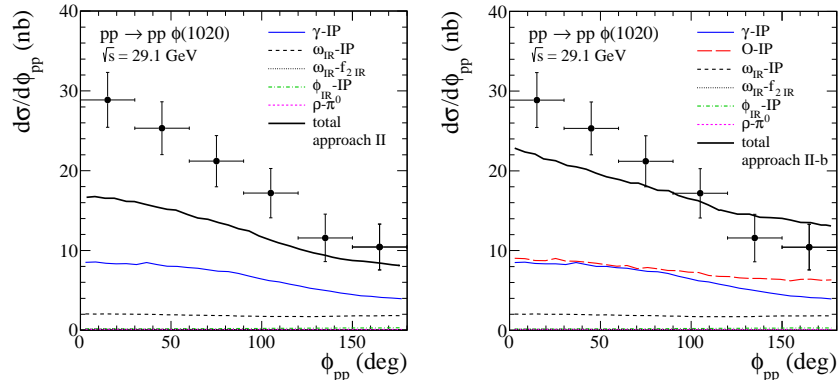


Fig. 3. The distributions in azimuthal angle  $\phi_{pp}$  between the transverse momentum vectors  $\mathbf{p}_{t,1}$ ,  $\mathbf{p}_{t,2}$  of the outgoing protons for  $\sqrt{s} = 29.1$  GeV together with the WA102 experimental data points normalized to the central value of the total cross section  $\sigma_{\text{exp}} = 60$  nb from [38]. In the left panel the results for the fusion processes  $\gamma\text{-IP}$ ,  $\omega_{\mathbb{R}}\text{-IP}$ ,  $\omega_{\mathbb{R}}\text{-}f_{2\mathbb{R}}$ ,  $\phi_{\mathbb{R}}\text{-IP}$ , and  $\rho\text{-}\pi^0$  are presented. The coherent sum of all terms is shown by the black solid line. In the right panel we added the  $\mathbb{O}\text{-IP}$  fusion term (see the red long-dashed line).

indicate a large interference effect between the  $\gamma\text{-IP}$ ,  $\mathbb{O}\text{-IP}$ ,  $\omega_{\mathbb{R}}\text{-IP}$ ,  $\omega_{\mathbb{R}}\text{-}f_{2\mathbb{R}}$ ,  $\phi_{\mathbb{R}}\text{-IP}$ , and  $\rho\text{-}\pi^0$  (for the reggeized  $\rho^0$ -meson exchange) terms. However, the subleading terms do not play a significant role at the LHC.

Having fixed the parameters of our model to the WA102 data we wish to show our predictions at  $\sqrt{s} = 13$  TeV for the LHC. Here we focus on the limited dikaon invariant mass region i.e., the  $\phi(1020)$  resonance region,  $1.01 \text{ GeV} < M_{K^+K^-} < 1.03 \text{ GeV}$ .

In Fig. 4 we show the results for the  $pp \rightarrow pp(\phi \rightarrow K^+K^-)$  reaction for experimental conditions relevant for ATLAS-ALFA or CMS-TOTEM ( $|\eta_K| < 2.5$ ,  $p_{t,K} > 0.1$  GeV, and with extra cuts on the leading protons of  $0.17 \text{ GeV} < |p_{y,1}|, |p_{y,2}| < 0.50$  GeV as will be the proton momentum window for the ALFA detectors) and at forward rapidities and without measurement of protons relevant for LHCb. The odderon-pomeron contribution dominates at larger  $p_{t,K^+K^-}$  and  $|y_{\text{diff}}|$  compared to the photon-pomeron contribution. For larger kaon transverse momenta (or transverse momentum of the  $K^+K^-$  pair) the odderon-exchange contribution is bigger than the photon-exchange one; see Table II of [31]. For the ATLAS-ALFA kinematics the absorption effects lead to a large damping of the cross sections both for the hadronic diffractive and for the photoproduction mechanisms.

Now we discuss the  $pp \rightarrow pp\mu^+\mu^-$  reaction for the LHCb kinematics ( $2.0 < \eta_\mu < 4.5$ ,  $p_{t,\mu} > 0.1$  GeV). Here we require no detection of the

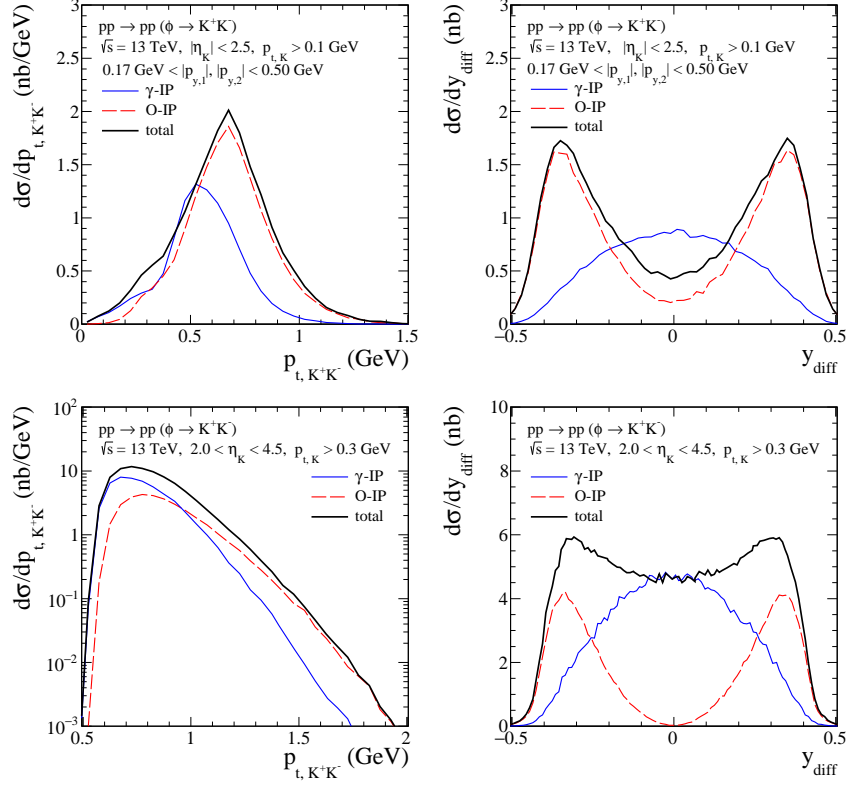


Fig. 4. The distributions in transverse momentum of the  $K^+K^-$  pair (left) and in rapidity difference between kaons  $y_{\text{diff}}$  for the  $pp \rightarrow pp(\phi \rightarrow K^+K^-)$  reaction. Shown are the  $\gamma$ - $\mathbb{P}$ - and  $\text{O}$ - $\mathbb{P}$ -fusion contributions and their coherent sum (denoted by “total”) for the ATLAS-ALFA (top) and the LHCb (bottom) experimental cuts.

leading protons. In contrast to dikaon production here there is for both the  $\gamma$ - $\mathbb{P}$ - and the  $\text{O}$ - $\mathbb{P}$ -fusion contributions a maximum at  $y_{\text{diff}} = 0$ . Imposing a larger cuts on the transverse momenta of the muons reduces the continuum ( $\gamma\gamma \rightarrow \mu^+\mu^-$ ) contribution which, however, still remains sizeable at  $y_{\text{diff}} = 0$ . The dimuon-continuum process ( $\gamma\gamma \rightarrow \mu^+\mu^-$ ) was discussed e.g. in [37] in the context of the ATLAS measurement.

Figure 5 shows the distributions in transverse momentum of the  $\mu^+\mu^-$  pair. We can see that the low- $p_{t,\mu^+\mu^-}$  cut can be helpful to reduce the continuum and  $\gamma$ - $\mathbb{P}$ -fusion contributions. In Fig. 6 we show the results when imposing in addition a cut  $p_{t,\mu^+\mu^-} > 0.8$  GeV. The  $\gamma\gamma \rightarrow \mu^+\mu^-$  contribution is now very small. We can see from the  $y_{\text{diff}}$  distribution that

the photon-pomeron term gives a broader distribution than the odderon-pomeron term. At  $y_{\text{diff}} = 0$  the odderon-exchange term is now bigger than the photoproduction terms.

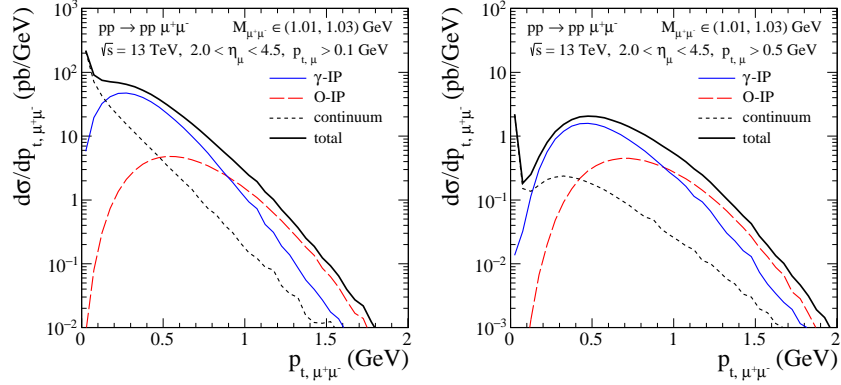


Fig. 5. The distributions in transverse momentum of the  $\mu^+\mu^-$  pair for the  $pp \rightarrow pp\mu^+\mu^-$  reaction in the dimuon invariant mass region  $M_{\mu^+\mu^-} \in (1.01, 1.03)$  GeV. Calculations were done for  $\sqrt{s} = 13$  TeV,  $2.0 < \eta_\mu < 4.5$ ,  $p_{t,\mu} > 0.1$  GeV (left) and for  $p_{t,\mu} > 0.5$  GeV (right). Results for the  $\phi$ -meson production via the  $\gamma$ - $\mathbb{P}$ - and the  $\mathbb{O}$ - $\mathbb{P}$ -fusion processes and the nonresonant  $\gamma\gamma \rightarrow \mu^+\mu^-$  continuum term are shown. Their coherent sum is shown by the black solid line.

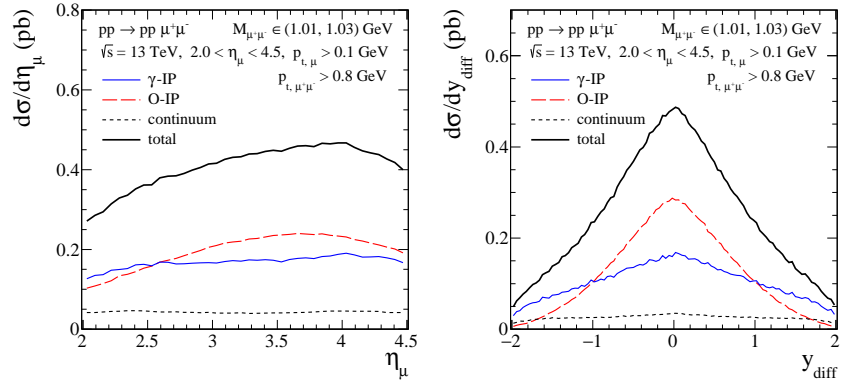


Fig. 6. The differential cross sections for the  $pp \rightarrow pp\mu^+\mu^-$  reaction in the dimuon invariant mass region  $M_{\mu^+\mu^-} \in (1.01, 1.03)$  GeV. Calculations were done for  $\sqrt{s} = 13$  TeV,  $2.0 < \eta_\mu < 4.5$ ,  $p_{t,\mu} > 0.1$  GeV, and  $p_{t,\mu^+\mu^-} > 0.8$  GeV. The meaning of the lines is the same as in Fig. 5.



In Fig. 7 we show two-dimensional distributions in  $(\eta_{\mu^+}, \eta_{\mu^-})$ . One can see quite different distributions for the  $\gamma$ - $\mathbb{P}$ - and the  $\mathbb{O}$ - $\mathbb{P}$  contributions. The odderon-exchange contribution shows an enhancement at  $\eta_{\mu^-} \sim \eta_{\mu^+} \sim 4$ .

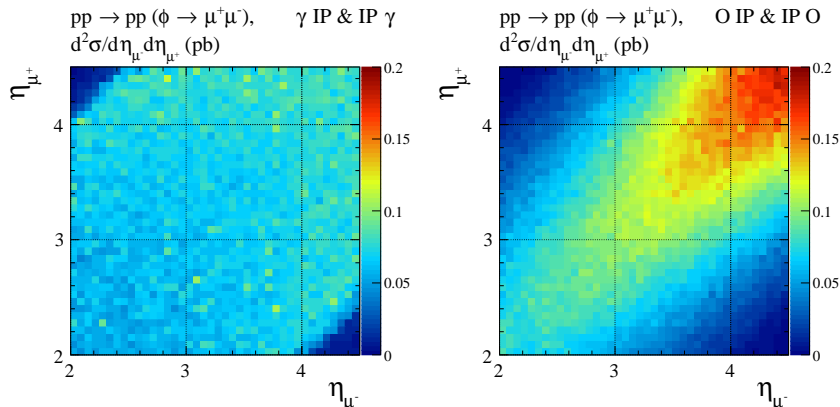


Fig. 7. The two-dimensional distributions in  $(\eta_{\mu^+}, \eta_{\mu^-})$  for the  $pp \rightarrow pp\mu^+\mu^-$  reaction. Shown are the results for the  $\phi$  production via  $\gamma$ - $\mathbb{P}$  fusion (left) and via  $\mathbb{O}$ - $\mathbb{P}$  fusion (right). The calculations were done for  $\sqrt{s} = 13$  TeV and with cuts on  $M_{\mu^+\mu^-} \in (1.01, 1.03)$  GeV,  $2.0 < \eta_{\mu} < 4.5$ ,  $p_{t,\mu} > 0.1$  GeV, and  $p_{t,\mu^+\mu^-} > 0.8$  GeV.

Now we go to the  $pp \rightarrow ppK^+K^-K^+K^-$  reaction. Fig. 8 shows the results including the  $f_2(2340)$ -resonance contribution and the continuum processes due to reggeized- $\phi$  and odderon exchanges. For the details how to calculate these processes see [30]. Inclusion of the odderon exchange improves the description of the WA102 data [39] for the  $pp \rightarrow pp\phi\phi$  reaction; see the left panel of Fig. 8. In the right panel we show the distribution in four-kaon invariant mass for the LHCb experimental conditions. The small intercept of the  $\phi$ -reggeon exchange,  $\alpha_\phi(0) = 0.1$  makes the  $\phi$ -exchange contribution steeply falling with increasing  $M_{4K}$ . Therefore, an odderon with an intercept  $\alpha_{\mathbb{O}}(0)$  around 1.0 should be clearly visible in the region of large  $M_{4K}$  (and also for large rapidity distance between the  $\phi$  mesons).

#### 4. Conclusions

We have discussed the possibility to search for odderon exchange in the  $pp \rightarrow pp\phi\phi$  and  $pp \rightarrow pp\phi$  reactions with the  $\phi$  meson observed in the  $K^+K^-$  or  $\mu^+\mu^-$  channels. For single  $\phi$  CEP at the LHC there are two basic processes: the relatively well known (at the Born level) photon-pomeron fusion and the rather elusive odderon-pomeron fusion. In this context the photon-pomeron fusion is a background for the odderon-pomeron fusion.

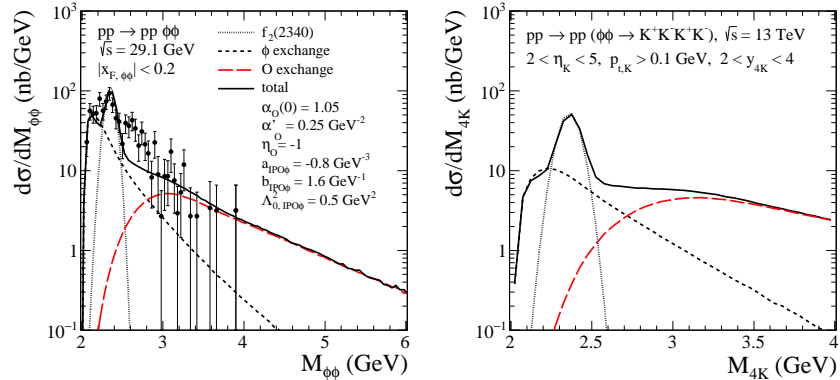


Fig. 8. The distributions in  $\phi\phi$  invariant mass (left) for  $\sqrt{s} = 29.1$  GeV and  $|x_{F,\phi\phi}| \leq 0.2$  and in  $M_{4K}$  (right) for  $\sqrt{s} = 13$  TeV and  $2 < \eta_K < 5$ ,  $2 < y_{4K} < 4$ ,  $p_{t,K} > 0.1$  GeV. The WA102 experimental data from [39] are shown. The black long-dashed line corresponds to the reggeized  $\phi$ -exchange contribution and the black dashed line corresponds to the  $f_2(2340)$  contribution. The red dashed line represents the odderon-exchange contribution. The coherent sum of all terms is shown by the black solid line.

The parameters of photoproduction were fixed to describe the HERA  $\phi$ -meson photoproduction data; see [31]. There, we pay special attention to the importance of the  $\phi$ - $\omega$  mixing effect.

To fix the parameters of the pomeron-odderon- $\phi$  vertex (coupling constants and cut-off parameters) we have considered several subleading contributions and compared our theoretical predictions for the  $pp \rightarrow pp\phi$  reaction with the WA102 experimental data from [38]. Having fixed the parameters of the model we have made estimates of the integrated cross sections as well as shown several differential distributions at the LHC; see Table II of [31]. In our opinion several distributions should be studied to draw a definite conclusion on the odderon exchange. For the  $\phi \rightarrow K^+K^-$  channel the distribution in  $y_{\text{diff}}$  (rapidity difference between kaons) seems particularly interesting. It is a main result of our analysis that, the  $y_{\text{diff}}$  distributions are very different for the  $\gamma$ - $\mathbb{P}$ - and  $\mathbb{O}$ - $\mathbb{P}$ -fusion processes. Observation of the pattern of maxima and minima would be interesting by itself as it is due to interference effects. This should be a big asset for an odderon search. The  $\mu^+\mu^-$  channel seems to be less promising in identifying the odderon exchange at least when only the  $p_{t,\mu}$  cuts are imposed. To observe a sizeable deviation from photoproduction, in the  $\phi \rightarrow \mu^+\mu^-$  channel, a  $p_{t,\mu^+\mu^-} > 0.8$  GeV cut on the transverse momentum of the  $\mu^+\mu^-$  pair seems necessary. A combined

analysis of both the  $K^+K^-$  and the  $\mu^+\mu^-$  channels should be the ultimate goal in searches for odderon exchange.

The  $pp \rightarrow pp\phi\phi$  process via odderon exchange shown in Fig. 2 (a) seems promising as here the odderon does not couple to protons. In our analysis on two  $\phi$ -meson production in proton-proton collisions [30] we tried to tentatively fix the parameters of the pomeron-odderon- $\phi$  vertex to describe the relatively large  $\phi\phi$  invariant mass distribution measured by the WA102 Collaboration [39]. Here we presented results for the odderon-exchange contribution with fixed the parameters of our model to the WA102 data [38] on  $pp \rightarrow pp\phi$ ; see Sec. IV A of [31]. We find from our model that the odderon-exchange contribution should be distinguishable from other contributions for relatively large rapidity separation between the  $\phi$  mesons. Hence, to study this type of mechanism one should investigate events with rather large four-kaon invariant masses, outside of the region of resonances. These events are then “three-gap events”: proton-gap- $\phi$ -gap- $\phi$ -gap-proton. Experimentally, this should be a clear signature.

We are looking forward to first experimental results on single and double  $\phi$  CEP at the LHC.

**Acknowledgments** I am indebted to Otto Nachtmann and Antoni Szczurek for collaboration on the issues presented here. This work was supported by the Polish National Science Centre grant 2018/31/B/ST2/03537.

## REFERENCES

- [1] L. Lukaszuk and B. Nicolescu, *Lett. Nuovo Cim.* **8** (1973) 405.
- [2] D. Joynson, E. Leader, B. Nicolescu, and C. Lopez, *Nuovo Cim.* **A30** (1975) 345.
- [3] J. Kwiciński and M. Praszalowicz, *Phys. Lett. B* **94** (1980) 413.
- [4] J. Bartels, *Nucl. Phys. B* **175** (1980) 365.
- [5] A. Breakstone *et al.*, *Phys. Rev. Lett.* **54** (1985) 2180.
- [6] G. Antchev *et al.*, (TOTEM Collaboration), *Eur. Phys. J. C* **79** (2019) 785.
- [7] G. Antchev *et al.*, (TOTEM Collaboration), *Eur. Phys. J. C* **80** (2020) 91.
- [8] E. Martynov and B. Nicolescu, *Phys. Lett.* **B778** (2018) 414; *Phys. Lett.* **B786** (2018) 207.
- [9] V. A. Khoze, A. D. Martin, and M. G. Ryskin, *Phys. Rev.* **D97** (2018) 034019; *Phys. Lett.* **B784** (2018) 192.
- [10] M. Broilo, E. Luna, and M. Menon, *Phys. Rev.* **D98** (2018) 074006.
- [11] A. Donnachie and P. V. Landshoff, arXiv:1904.11218 [hep-ph].
- [12] A. Schäfer, L. Mankiewicz, and O. Nachtmann, *Phys.Lett.* **B272** (1991) 419.
- [13] A. Bzdak, L. Motyka, L. Szymanowski, and J.-R. Cudell, *Phys.Rev.* **D75** (2007) 094023, arXiv:hep-ph/0702134 [hep-ph].

- [14] A. Schäfer, L. Mankiewicz, and O. Nachtmann, Diffractive  $\eta_c$ ,  $\eta'$ ,  $J/\psi$  and  $\psi'$  production in electron-proton collisions at HERA energies, in *the proceedings of the workshop on Physics at HERA, Hamburg, Germany, October 29-30, 1991*, p. 243. W. Buchmüller and G. Ingelman (eds.) DESY, 1992.
- [15] V. V. Barakhovsky, I. R. Zhitnitsky, and A. N. Shelkovenko, Phys. Lett. **B267** (1991) 532.
- [16] W. Kilian and O. Nachtmann, Eur. Phys. J. **C5** (1998) 317.
- [17] E. R. Berger, A. Donnachie, H. G. Dosch, W. Kilian, O. Nachtmann, and M. Rüeter, Eur.Phys.J. **C9** (1999) 491, arXiv:hep-ph/9901376 [hep-ph].
- [18] E. R. Berger, A. Donnachie, H. G. Dosch, and O. Nachtmann, Eur. Phys. J. **C14** (2000) 673, arXiv:hep-ph/0001270 [hep-ph].
- [19] A. Donnachie, H. G. Dosch, and O. Nachtmann, Eur.Phys.J. **C45** (2006) 771.
- [20] C. Ewerz and O. Nachtmann, Eur.Phys.J. **C49** (2007) 685.
- [21] C. Ewerz, arXiv:hep-ph/0306137 [hep-ph].
- [22] V. P. Goncalves, Eur. Phys. J. **C79** (2019) 408.
- [23] L. A. Harland-Lang, V. A. Khoze, A. D. Martin, and M. G. Ryskin, Phys. Rev. **D99** (2019) 034011.
- [24] V. P. Goncalves and W. K. Sauter, Phys. Rev. **D91** (2015) 094014.
- [25] C. Ewerz, M. Maniatis, and O. Nachtmann, Annals Phys. **342** (2014) 31.
- [26] A. Bolz, C. Ewerz, M. Maniatis, O. Nachtmann, M. Sauter, and A. Schönig, JHEP **1501** (2015) 151, arXiv:1409.8483 [hep-ph].
- [27] P. Lebiedowicz, O. Nachtmann, and A. Szczurek, Annals Phys. **344** (2014) 301; Phys. Rev. **D91** (2015) 074023; Phys. Rev. **D93** (2016) 054015; Phys. Rev. **D94** (2016) 034017; Phys. Rev. **D95** (2017) 034036; Phys. Rev. **D101** (2020) 034008.
- [28] Phys. Rev. **D97** (2018) 094027, arXiv:1801.03902 [hep-ph].
- [29] P. Lebiedowicz, O. Nachtmann, and A. Szczurek, Phys. Rev. **D98** (2018) 014001, arXiv:1804.04706 [hep-ph].
- [30] P. Lebiedowicz, O. Nachtmann, and A. Szczurek, Phys. Rev. **D99** (2019) 094034, arXiv:1901.11490 [hep-ph].
- [31] P. Lebiedowicz, O. Nachtmann, and A. Szczurek, arXiv:1911.01909 [hep-ph].
- [32] C. Ewerz, P. Lebiedowicz, O. Nachtmann, and A. Szczurek, Phys. Lett. **B763** (2016) 382, arXiv:1606.08067 [hep-ph].
- [33] L. Adamczyk *et al.*, (STAR Collaboration), Phys. Lett. **B719** (2013) 62.
- [34] D. Britzger, C. Ewerz, S. Glazov, O. Nachtmann, and S. Schmitt, Phys. Rev. **D100** (2019) 114007, arXiv:1901.08524 [hep-ph].
- [35] A. Donnachie, H. G. Dosch, P. V. Landshoff, and O. Nachtmann, Camb.Monogr.Part.Phys.Nucl.Phys.Cosmol. **19** (2002) 1.
- [36] P. Lebiedowicz and A. Szczurek, Phys. Rev. **D92** (2015) 054001.
- [37] P. Lebiedowicz and A. Szczurek, Phys. Rev. **D98** (2018) 053007.
- [38] A. Kirk, Phys.Lett. **B489** (2000) 29, arXiv:0008053 [hep-ph].
- [39] D. Barberis *et al.*, (WA102 Collaboration), Phys. Lett. **B432** (1998) 436.